Journal of Medicinal Chemistry

Article

Cite This: J. Med. Chem. 2018, 61, 6153−6162

pubs.acs.org/jmc

New Analogs of the Complement C3 Inhibitor Compstatin with Increased Solubility and Improved Pharmacokinetic Profile

Nadja Berger,[†] Tchilabalo Dilezitoko Alayi,[†] Ranillo R. G. Resuello,[‡] Joel V. Tuplano,[‡] Edimara S. Reis,[†] and John D. Lambris*[,†]

[†]Department of Pathology and Laboratory Medicine, Perelman School of Medicine, University of Pennsylvania, Philadelphia, Pennsylvania 19104, United States

[‡]Simian Conservation Breeding and Research Center (SICONBREC), Makati City 1231, Philippines

Supporting Information

ABSTRACT: Improper regulation of complement is associated with various pathologies, and the clinical demand for compounds that can regulate complement activation is therefore imperative. Cp40, an analog of the peptide compstatin, inhibits all complement pathways at the level of the central component C3. We have further developed Cp40, using either PEGylation at the N-terminus or insertion of charged amino acids at the C-terminus. The PEGylated analogs are highly soluble and retained their inhibitory activity, with C3b binding affinity dependent on the length of the PEG chain. The addition of two or three residues of lysine, in turn, not only improved the peptide's solubility but also increased the binding affinity for C3b while retaining its inhibitory potency. Three of the new derivatives showed improved pharmacokinetic profiles in vivo in non-human primates. Given their compelling solubility and pharmacokinetic profiles, these new Cp40 analogs should broaden the spectrum of administration routes, likely reducing dosing frequency during chronic treatment and potentially expanding their range of clinical application.

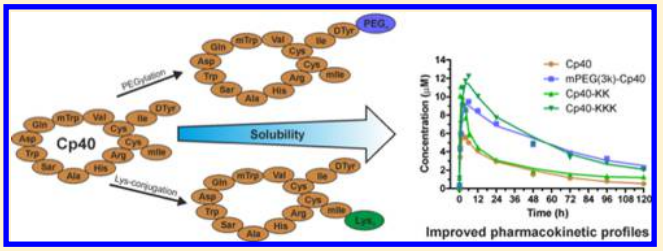

INTRODUCTION

Aberrant activation of the complement system is associated with a variety of inflammatory, autoimmune, and neurodegenerative diseases, as well as cancer, sepsis, hemorrhagic shock, and complications resulting from hemodialysis and transplantation.[1−8] Despite tremendous ongoing efforts in research and drug development in this field, a humanized monoclonal antibody against C5 (eculizumab) that prevents its cleavage and subsequent activation of the terminal pathway of complement remains the only complement-specific therapeutic available in the clinic for the treatment of paroxysmal nocturnal hemoglobinuria (PNH) and atypical hemolytic uremic syndrome (aHUS).[9,10] Nevertheless, a considerable number of drug candidates designed to intervene at different stages of the complement cascade, including small molecules, peptides, proteins, antibodies, and oligonucleotides, are currently in preclinical and clinical phases of development.[11−14]

Among possible points of therapeutic intervention, upstream inhibition at the level of C3, the central component of the complement cascade, has been explored as an attractive approach, given the involvement of C3 and its downstream activation fragments in a variety of immune and inflammatory mechanisms that exacerbate pathology in a wide spectrum of clinical disorders.[4] In fact, substantial progress in the development of clinical C3 inhibitors has been achieved in recent years.[15]

The compstatin family, a group of cyclic peptides consisting of ∼13 amino acids, shows highly selective and strong binding affinity to human C3 and its fragments C3b and C3c and to non-human primate (NHP) C3, preventing complement activation.[15−17] The most potent derivative, Cp40, has a subnanomolar binding affinity for C3b and extended plasma half-life.[18,19] Most importantly, Cp40 showed promising therapeutic efficacy when used in NHP models of periodontitis, hemodialysis, kidney transplantation, and hemorrhagic shock.[11,15,20,21] While a successful phase I trial with the Cp40-based drug candidate AMY-101 (Amyndas Pharmaceuticals) has recently been completed, other compstatin analogs (APL-2, which is the PEGylated version of POT-4, also known as 4(1MeW)7W or APL-1; Apellis Pharmaceuticals) are currently being evaluated in clinical studies for the treatment of age-related macular degeneration (AMD), PNH, and glomerulopathies.[11,14,22−26]

Here, we introduce new analogs of Cp40 with enhanced solubility and improved pharmacokinetic profiles. PEGylation or the addition of Lys residues was successfully used to increase the solubility of Cp40 at physiological pH (∼7.4). The favorable C3 inhibitory activity of Cp40 was unaffected by these modifications, and the binding affinity of the Lys derivatives toward C3b was even stronger than that of the

Received: April 9, 2018
Published: June 19, 2018

DOI: 10.1021/acs.jmedchem.8b00560
J. Med. Chem. 2018, 61, 6153−6162

parental compound Cp40. In addition, the new Cp40 variants showed similar or prolonged half-lives after subcutaneous (sc) administration into NHPs, resulting in longer saturation of plasma C3 (period of time in which the molar concentration of a Cp40 analog is equal to or above the molar concentration of plasma C3) when compared with Cp40. These improved properties facilitate sc administration of the Cp40 variants, thereby leveraging patient compliance during chronic C3-targeted intervention in clinical trials, and may also expand the possible routes for Cp40 delivery, thus widening its potential use in various indications.

RESULTS

Design of Cp40 Analogs with Enhanced Solubility. Among the peptides of the compstatin family, the analog Cp40 is the most promising drug candidate because of its high target affinity and favorable pharmacokinetic profile. However, despite its high solubility in water, it shows poor solubility at physiological pH (0.8 mg/mL).[19] Therefore, we aimed to modify Cp40 to improve its solubility without losing its inhibitory activity or binding affinity for C3b. In accordance with previous findings, neither the N- nor the C-terminus of Cp40 is involved in the binding to C3.[19,27] Thus, modifications to enhance the peptide's solubility were attempted on the terminal regions of Cp40.

We have previously attached a long polyethylene glycol chain (40 kDa) at either the C- or N-terminus of Cp40. PEGylation of the N-terminus, but not C-terminus of Cp40, extended the peptide's residence time in plasma after in vivo administration in NHP.[28] Notably, PEGylation of the N-terminus did not significantly change the biochemical properties of Cp40, largely retaining the inhibitory activity of unmodified Cp40. On the basis of these results, we set out to attach shorter PEG chains (of 3, 2, and 1 kDa) to the N-terminus of Cp40 via amide coupling. The resulting analogs were termed mPEG(3k)-Cp40, mPEG(2k)-Cp40, and mPEG-(1k)-Cp40 (Figure 1). PEGylation drastically increased the solubility of the resulting Cp40 analogs, with mPEG(3k)-Cp40 showing solubility of >270 mg/mL in PBS (Table 1). The size of the PEG chain was directly associated with compound solubility, with the solubility of mPEG(3k)-Cp40 > mPEG-(2k)-Cp40 > mPEG(1k)-Cp40 > Cp40 (Table 1).

PEGs are polymers usually available as polydisperse compounds. Since compounds with a well-defined structure are more uniform and can be better characterized,[29] we were interested in PEGylating Cp40 using monodisperse polymers. As such, analogs containing monodisperse mPEG(1056) and mPEG(528) were also synthesized. While the solubility of mPEG(1056)-Cp40 was similar to that of its polydisperse counterpart, attachment of a shorter PEG chain (528 Da) resulted in a significant decrease in the compound solubility in PBS, from 137 to 2.3 mg/mL (almost as low as that of unmodified Cp40, Table 1).

In addition to PEGylation, incorporation of hydrophilic/charged residues was used as an alternative approach to increase the solubility of Cp40.[30] To this end, one, two, or three lysine residues were attached to the C-terminus of Cp40 during peptide synthesis. Notably, peptide solubility increased with an increasing number of Lys residues; i.e., the solubility of Cp40-K (7.1 mg/mL) was lower than that of Cp40-KK and Cp40-KKK (>245 mg/mL) (Table 1). Interestingly, whereas a pH of ~7.5 was measured in a PBS solution containing 277 mg/mL of Cp40-KK, similar concentration of Cp40-KKK resulted in a solution with an increased pH of 8.5 (Table 1), reflecting the basic properties of the Lys residue.

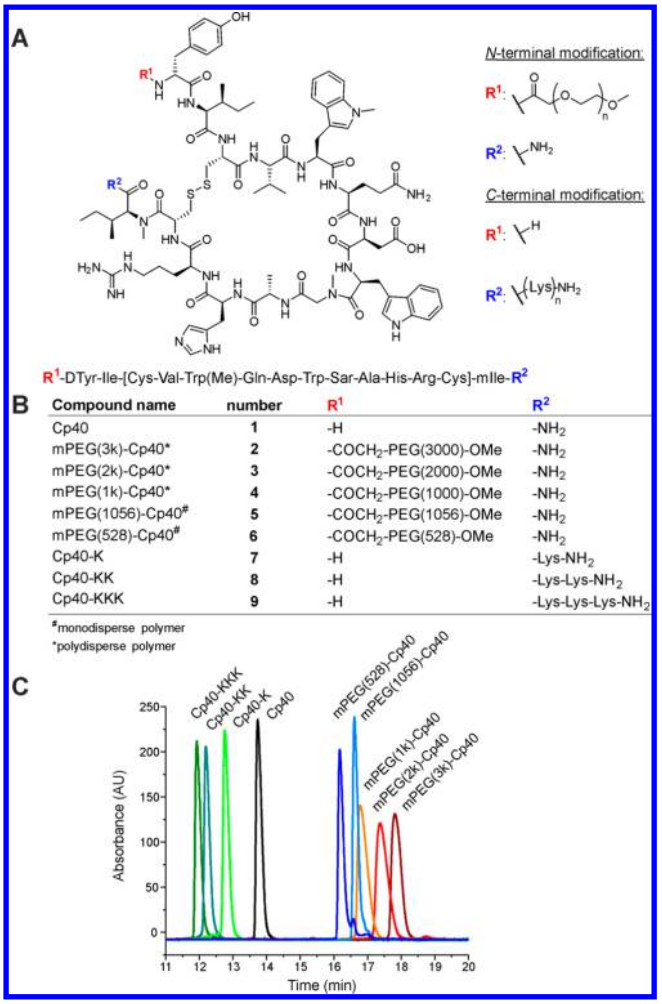

Figure 1. Novel Cp40 analogs: (A) general structure of Cp40 as well as N- and C-terminal modifications of the new analogs; (B) new Cp40 analogs containing mPEG or Lys modifications at the N (R^1) or C (R^2) terminus, respectively; (C) graph depicting excerpts of the UV–HPLC chromatograms showing Cp40 and its analogs eluting between 11.9 and 17.8 min (see Figure S5 for full chromatograms).

Table 1. Solubility and pH of the Solution Containing the Cp40 analogs[a]

analog	concentration (mg/mL)	pH
Cp40	1.08	7.5
mPEG(3k)-Cp40	>270	7
mPEG(2k)-Cp40	172	7.5
mPEG(1k)-Cp40	157	~7.5
mPEG(1056)-Cp40	137	~7.5
mPEG(528)-Cp40	2.3	~7.5
Cp40-K	7.1	7.5
Cp40-KK	277	~7.5
Cp40-KKK	>245	8.5

[a]">" indicates that saturation was not achieved in the specified concentration.

Complement Inhibitory Potency and Target Affinity of New Cp40 Derivatives. To verify that the modified peptides retained Cp40's complement inhibitory activity and target affinity, we evaluated inhibition of classical pathway

DOI: 10.1021/acs.jmedchem.8b00560
J. Med. Chem. 2018, 61, 6153–6162

Table 2. Complement Inhibition Potency and Kinetic Parameters of Cp40 Analogs[a]

analog	IC_{50} (nM)	k_a (10^6 M^{-1} s^{-1})	k_d (10^{-3} s^{-1})	K_D (nM)
Cp40	56.8 ± 3.0	3.57 ± 0.70	1.84 ± 0.40	0.53 ± 0.14
mPEG(3k)-Cp40	83.0 ± 7.0	0.45 ± 0.27	2.40 ± 0.91	7.91 ± 2.02
mPEG(2k)-Cp40	83.8 ± 4.5	0.54 ± 0.13	2.39 ± 0.46	4.47 ± 0.61
mPEG(1k)-Cp40	52.7 ± 2.9	0.76 ± 0.15	2.18 ± 0.14	2.98 ± 0.54
mPEG(1056)-Cp40	52.0 ± 2.7	0.72 ± 0.25	2.80 ± 0.95	3.93 ± 0.39
mPEG(528)-Cp40	83.5 ± 8.1	1.00 ± 0.27	2.45 ± 0.28	2.58 ± 0.51
Cp40-K	95.6 ± 9.2	1.98 ± 0.20	1.85 ± 0.50	0.92 ± 0.20
Cp40-KK	61.8 ± 4.2	3.94 ± 1.26	1.52 ± 0.25	0.44 ± 0.17
Cp40-KKK	81.7 ± 5.3	3.83 ± 2.58	1.24 ± 0.42	0.21 ± 0.09

[a] IC_{50} values of Cp40 analogs were assessed by classical pathway complement inhibition assay.[31] Association constant (k_a), dissociation constant (k_d), and equilibrium dissociation constant (K_D) were determined by surface plasmon resonance (SPR) experiments. Values show the mean ± standard deviation calculated from three independent experiments.

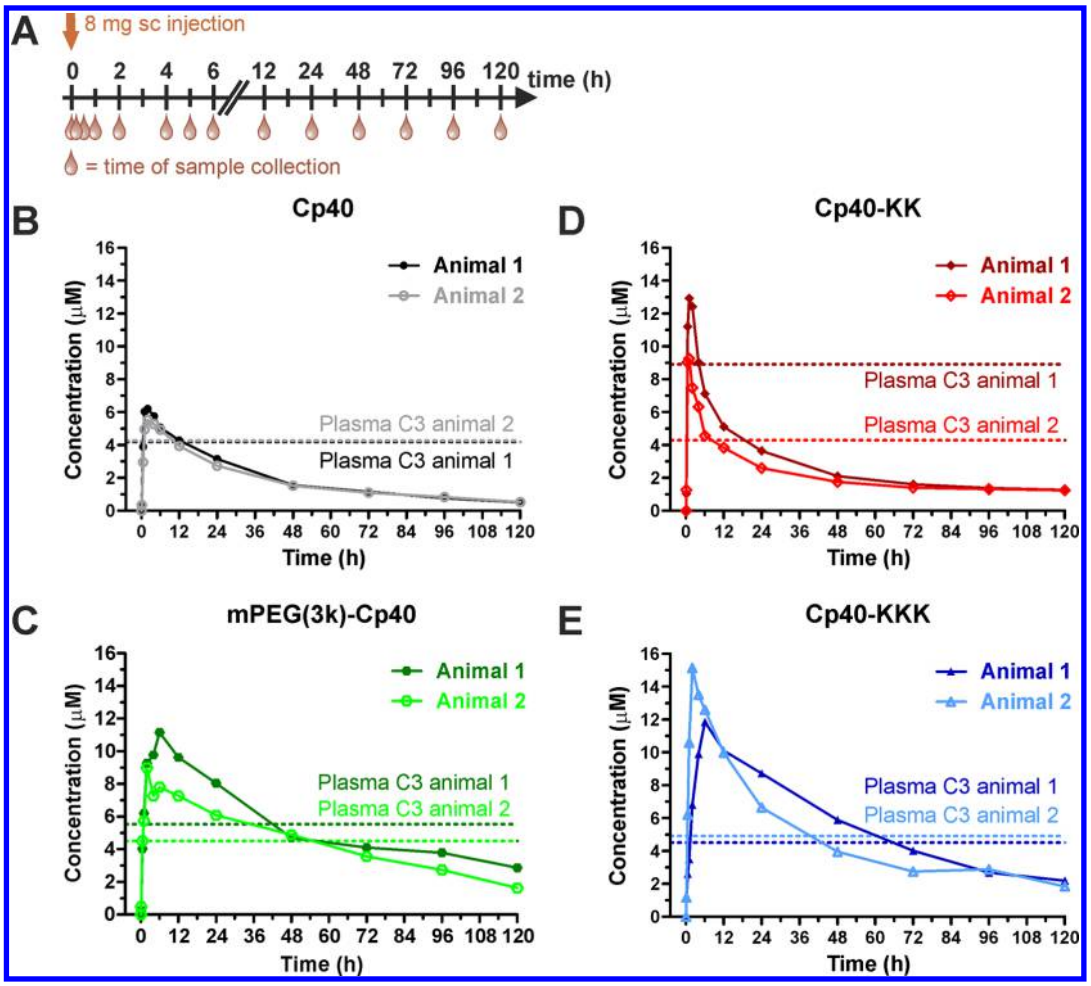

Figure 2. Pharmacokinetic evaluation of Cp40 and its new analogs in vivo in NHP. (A) Schematics showing a single-dose administration of peptide via sc injection into cynomolgus monkeys (n = 2 per treatment group) at 0 h (brown arrow). Cp40 (8 mg net) was administered into each monkey (2 mg/kg), and blood samples were collected at various time points (red drops). (B–E) Pharmacokinetic profiles of Cp40 (B), mPEG(3k)-Cp40 (C), Cp40-KK (D), and Cp40-KKK (E), as assessed by UPLC-ESI-MS analysis of the NHP plasma samples. C3 levels in each animal are shown in corresponding colors as dotted lines. Graph depicts total concentrations of Cp40-KK (Cp40-KK plus cleavage product Cp40-K) and Cp40-KKK (Cp40-KKK plus cleavage products Cp40-KK and Cp40-K). Individual quantification of original compounds and cleavage products is shown in Figure S4.

complement activity in an in vitro immune complex-induced complement activation assay.[31] Indeed, the inhibitory activity of the peptide was not significantly influenced by PEGylation at the N-terminus or the addition of Lys residues at the C-terminus (Table 2 and Figure S1), thus corroborating previous structure–function studies that had revealed that both termini of compstatin can tolerate structural modifications without any negative impact on its inhibitory mode.[19]

In contrast, the binding affinity of the individual peptides to C3b was affected by the nature of the modifications added to Cp40 (Table 2). Whereas the addition of the shortest PEG chain to the N-terminus of Cp40 (mPEG(528)-Cp40) resulted

DOI: 10.1021/acs.jmedchem.8b00560
J. Med. Chem. 2018, 61, 6153–6162

Table 3. Pharmacokinetic Parameters of Cp40 Analogs[a]

analog	animal	$t_{1/2}$ (h)	t_{max} (h)	C_{max} (μM)	AUC_{0-120h} (μM h)	AUC_{inf} (μM h)	Vz/F (mL/kg)	CL/F (mL h^{-1} kg^{-1})
Cp40	1	40.9	2	6.20	233	263	448 946	7605
	2	48.1	2	5.53	218	255	545 665	7856
Cp40-KK	1	145	1	12.90	329	597	700 664	3348
	2	276	1	9.26	257	755	1 055 443	2648
Cp40-KKK	1	46.7	6	11.90	658	805	167 382	2483
	2	41.8	2	15.10	573	685	176 010	2921
mPEG(3k)-Cp40	1	64.8	6	11.10	654	922	202 917	2169
	2	53.7	2	8.99	529	656	236 127	3050

[a]Pharmacokinetic parameters obtained after sc injection of Cp40 analogs in NHPs (n = 2 per treatment group). Cp40-KK and Cp40-KKK: parameters calculated for total active peptide (original compound plus cleavage products). $t_{1/2}$, terminal half-life; t_{max}, time at which C_{max} is observed; C_{max}, maximum concentration; AUC, area under the curve; Vz/F, apparent volume of distribution (F = bioavailability); CL/F, apparent clearance.

in a 5-fold decrease (K_D = 2.45 nM) of the binding affinity toward C3b, increasing the length of the PEG chain further reduced the affinity of mPEG(3k)-Cp40 (K_D = 7.9 nM) as compared to that of Cp40 (K_D 0.5 nM) (Table 2, Figures S2 and S3). In contrast, attachment of Lys residues increased the binding of the resulting analogs to C3b. Whereas the addition of a single Lys residue did not affect the binding significantly, addition of two or three Lys residues resulted in a 1.2- and 2.5-fold increase in the binding affinity to C3b, respectively (Table 2, Figures S2 and S3). Overall, the variation in the dissociation rate ($(1.24-2.8) \times 10^{-3}$ s^{-1}) of the various analogs was lower than that of the association rate ($(0.45-3.94) \times 10^{6}$ M^{-1} s^{-1}).

Pharmacokinetic Analysis of Cp40 Analogs in Plasma of Non-Human Primates. The new Cp40 analogs as well as the parent molecule were then tested in vivo in NHPs to assess the influence of PEGylation and Lys conjugation on their pharmacokinetic profiles. The compounds mPEG(3k)-Cp40, Cp40-KK, and Cp40-KKK were selected for the in vivo studies because of their improved solubility. Each peptide was injected subcutaneously in a single dose (2 mg/kg) into two monkeys, and blood samples were collected over a period of 5 days (Figure 2A).

A single sc injection of Cp40 resulted in an immediate increase of the peptide plasma levels, with a maximum concentration ($C_{max} \approx 5.9$ μM, mean value calculated from data obtained from two animals) at 2 h postinjection (Figure 2B and Table 3), followed by a slow elimination phase, resulting in an area under the curve AUC_{0-120h} of ~226 μM h, an apparent clearance CL/F of ~7,730 mL h^{-1} kg^{-1}, and a terminal half-life ($t_{1/2}$) of ~44.5 h (Figure 2B and Table 3). Notably, the observed $t_{1/2}$ was longer than that obtained in an earlier study ($t_{1/2}$ ~12 h), in which cynomolgus monkeys were also dosed with 2 mg/kg of Cp40 sc.[19] This apparent discrepancy is attributed to the different observation periods (5 days here vs 1 day), since shorter observation periods do not allow for precise calculations of $t_{1/2}$.

The UPLC-ESI-MS quantification method previously established by our group[19,32] was modified and further developed for the quantification of mPEG(3k)-Cp40. Since the mPEG(3k) chain was polydisperse and no single peak could be detected by ESI-MS, we applied a fixed collision energy of 35 V in the ion trap to produce a monocharged mass peak at 436.259 m/z, which could be assigned to the fragment -Sar-Ala-His-Arg- of mPEG(3k)-Cp40. The mass of this fragment was used to process and analyze the plasma samples containing mPEG(3k)-Cp40 similarly to those containing Cp40. A single sc injection of mPEG(3k)-Cp40 in monkeys resulted in a pharmacokinetic profile comparable to that obtained for administration of the parental compound Cp40, with a t_{max} at 2–6 h postinjection (Figure 2B,C). Despite the similar pharmacokinetic curve, mPEG(3k)-Cp40 reached a C_{max} of ~10 μM, almost 2-fold higher than the parental peptide (Figure 2C and Table 3). Furthermore, the AUC_{0-120h} (~592 μM h) was higher, the $t_{1/2}$ (~59 h) was longer, and the CL/F (~2610 mL h^{-1} kg^{-1}) was slower than the respective values obtained for Cp40 (Table 3). In addition, the target protein C3 was saturated for a longer period of time (~34 h vs ~4.5 h for Cp40) (Figure 2B,C).

In contrast to Cp40 and mPEG(3k)-Cp40, Cp40-KK showed a C_{max} of ~11 μM in the plasma 1 h after administration, $t_{1/2}$ of ~210 h, AUC_{0-120h} of ~293 μM h, and CL/F of ~3000 mL h^{-1} kg^{-1} (Figure 2D, Table 3). As previously reported,[19] the pharmacokinetic behavior of Cp40 follows a target-driven elimination model, and this is corroborated in the case of Cp40-KK; the peptide C_{max} is associated with the plasma concentrations of C3 (Figure 2B,D). Of note, Figure 2D illustrates the quantification of total active peptide, i.e., Cp40-KK plus the cleavage product Cp40-K. Although in small quantity, Cp40-K was detected at a constant amount in the plasma of injected animals, beginning at 30 min postinjection, thereby suggesting that enzymatic cleavage of the peptide's terminal Lys residue occurs in vivo (Figure S4A,B).

Sterile saline was used as a vehicle for all the compounds except Cp40-KKK. Since the addition of three Lys residues resulted in a compound with basic characteristics, sterile phosphate solution was used to buffer the injection suspension at pH ~7.5. As detailed above for Cp40-KK, the pharmacokinetic profile of the total active peptide is shown in Figure 2E, i.e., Cp40-KKK plus the cleavage products Cp40-KK and Cp40-K. The pharmacokinetic profiles of the individual cleavage products are shown in Figure S4C,D. The single injection of Cp40-KKK resulted in a pharmacokinetic profile comparable to those of Cp40 and mPEG(3k)-Cp40. The peptide reached a C_{max} of ~13.5 μM at 2–6 h postinjection (Figure 2E and Table 3), with an AUC_{0-120h} of ~616 μM h, CL/F of ~2700 mL h^{-1} kg^{-1}, and $t_{1/2}$ of ~44.3 h. In addition, after the administration of Cp40-KKK, plasma levels of C3 remained saturated for ~40 h; 7-fold longer than the saturation period observed with unmodified Cp40 (Figure 2E).

Evaluation of the individual peptide metabolites present in plasma revealed low amounts of the intact Cp40-KKK during the observation time, significant amounts of Cp40-KK

DOI: 10.1021/acs.jmedchem.8b00560
J. Med. Chem. 2018, 61, 6153–6162

(~70%), and minimum amounts of Cp40-K (reaching plasma concentrations as high as 5 μM) (Figure S4C,D). These data suggest a rapid cleavage of Cp40-KKK to Cp40-KK and Cp40-K upon injection.

DISCUSSION

In the present study, we have developed and characterized new analogs of the C3 inhibitor Cp40 that showed increased solubility and improved pharmacokinetic profile while retaining the activity and target affinity of the parental peptide.

Cp40, albeit showing strong activity and a favorable pharmacokinetic profile in vivo, demonstrated low solubility (~0.8 mg/mL) at pH ~7.0.[19] Because compounds that are highly soluble at physiological pH would facilitate administration by different routes (i.e., intravitreal, intravenous, or subcutaneous), allow higher dosages, longer dosing intervals, and potentially avoid any precipitation,[33] we set out to develop analogs with increased solubility. Indeed, previous studies have demonstrated the substantial effects of small modifications in a peptide, not only on its efficacy but also on its physicochemical properties such as solubility.[19,34−37] Here, the C-terminus and N-terminus of Cp40 were chosen as points of modification, avoiding any modification within the core structure (ring) that is responsible for the peptide's activity.[19,27]

The conjugation of relatively short polymers, namely mPEG(1k), mPEG(2k), and mPEG(3k), to Cp40 drastically increased the solubility of the parent peptide. The length of the PEG chain was the final determinant of solubility, with the 1 kDa mPEG being the shortest chain that was able to increase the solubility of Cp40 (Table 1). Since the polydisperse nature of the PEG polymers hampers the characterization of the compounds, we have shown here that the use of monodisperse PEGs circumvents this difficulty.[29,38] Furthermore, we found that monodisperse PEG could be conjugated to the N-terminus of the peptide during solid-phase peptide synthesis without additional steps, thereby improving the synthesis reproducibility.[39]

One of the potential primary risks to be considered with therapeutic PEGylated compounds is the development of immunogenicity in vivo.[40] Indeed, anti-PEG antibodies have been observed in clinical studies and are correlated with the loss of therapeutic efficacy.[41−43] In such cases, however, high molecular weight PEGs (≥5 kDa) were used in an attempt to prevent peptide degradation in vivo and extend its residence time in the body.[44] In addition, the use of large-size PEGs (>20 kDa) has been associated with adverse effects such as cellular vacuolation or increased toxicity due to accumulation within the liver or decreased renal clearance.[44] It is anticipated that such issues are not a concern in the case of PEGylated Cp40 due to the significantly shorter size of PEGs used in this study.

In addition to PEGylation, the attachment of Lys residues to the C-terminus of Cp40 also increased the peptide's solubility (Table 1). Whereas the Cp40 N-terminal modification by conjugation of mPEG resulted in a 3- to 6-fold decrease in the association constant (k_a) with C3b, no significant change was observed in the dissociation constant (k_d) when compared to the parental compound, Cp40. The lower k_a values were reflected in lower affinity values, especially for the analogs carrying longer PEG chains (mPEG(3k)-Cp40, 7.9 nM; mPEG(2k)-Cp40, 4.4 nM), when compared with Cp40 (K_D = 0.5 nM). The apparent lower affinity, however, did not significantly affect the activity of the analogs (Table 2). It is likely that this apparent discrepancy results from the different specificity of the methods used, as the SPR analysis offers more quantitative data when compared with the IC_{50} values obtained by ELISA.[18,19] Similarly, the addition of Lys residues to Cp40 did not significantly influence any of the biochemical parameters mentioned above, indicating that the chosen modifications did not induce major changes in the interaction between the analogs and C3 (Table 2).

The analogs mPEG(3k)-Cp40, Cp40-KK, and Cp40-KKK showed the highest solubility at pH ~7.5 (>245 mg/mL) and were tested in vivo as a single sc injection of 2 mg/kg in cynomolgus monkeys. Interestingly, injection of these analogs resulted in approximately doubling the C_{max} value when compared to that obtained for unmodified Cp40, with C_{max} for Cp40 < mPEG(3k)-Cp40 < Cp40-KK < Cp40-KKK (Table 3). In addition to improvements in C_{max}, the terminal half-life of the compound was also extended from 44.5 to 59 h, with $t_{1/2}$ for Cp40 ~ Cp40-KKK < mPEG(3k)-Cp40 < Cp40-KK. (Table 3). Improved pharmacokinetics of the new analogs were also reflected in their increased AUC_{0-120h} (Cp40 < Cp40-KK < mPEG(3k)-Cp40 < Cp40-KKK) and slower CL/F (Cp40 > Cp40-KK > mPEG(3k)-Cp40 ~ Cp40-KKK). In addition, the time of C3 saturation was extended (Cp40 ~ Cp40-KK < mPEG(3k)-Cp40 < Cp40-KKK). Overall, when compared with the parental peptide Cp40, the new analogs maintain the inhibitory activity and show increased solubility, C_{max}, longer terminal half-life and slower drug clearance, favoring extended dosing intervals. The pharmacokinetics evaluation indicates a similar profile between Cp40-KKK and mPEG(3k)-Cp40, with a t_{max} of 2−6 h, followed by slow clearance and 48 h of target saturation. These data point toward slower release of these compounds from the subcutaneous compartment into the circulation, potentially contributing to longer saturation of the circulating C3. The Cp40-KK analog, in turn, shows a different biphasic elimination kinetics reaching an early t_{max} at 1 h postinjection followed by a rapid initial clearance and a slower elimination in the terminal phase, resulting in 8−12 h of target saturation.

Although the association rate and binding affinity of mPEG(3k)-Cp40 was lower, the dissociation rate of all the derivatives was very similar, and the higher solubility of mPEG(3k)-Cp40 resulted in a higher C_{max}, determining the overall pharmacokinetic behavior. In contrast to mPEG(3k)-Cp40 and Cp40, Cp40-KK was quickly absorbed into the circulation. The C_{max} reached was also higher than that of unmodified Cp40, which could be explained by the high solubility of Cp40-KK. Soon after the C_{max} peak, Cp40-KK clearance began rapidly but slowed over time resulting in an extended $t_{1/2}$ when compared to that of the parental peptide. Unlike the rapid absorption of Cp40-KK, Cp40-KKK absorption into the circulatory system was slower and its pharmacokinetics was more favorable, with AUC_{0-120h} and CL/F values similar to those of mPEG(3k)-Cp40.

Interestingly, Lys cleavage products were detected in the plasma of animals injected with Cp40-KK and Cp40-KKK, indicating the occurrence of enzymatic cleavage in vivo. Indeed, incubation of Cp40-KK or Cp40-KKK with monkey or human plasma in vitro resulted in the cleavage of the C-terminal Lys (Figure 3). Cleavage of Cp40-KK into Cp40-K was observed both in vivo after injection in NHPs (Figure S4) and in vitro after incubation with NHP or human plasma (Figure 3). In contrast, Cp40-KKK was mainly cleaved into Cp40-KK in vivo while in vitro studies using NHP or human

DOI: 10.1021/acs.jmedchem.8b00560
J. Med. Chem. 2018, 61, 6153−6162

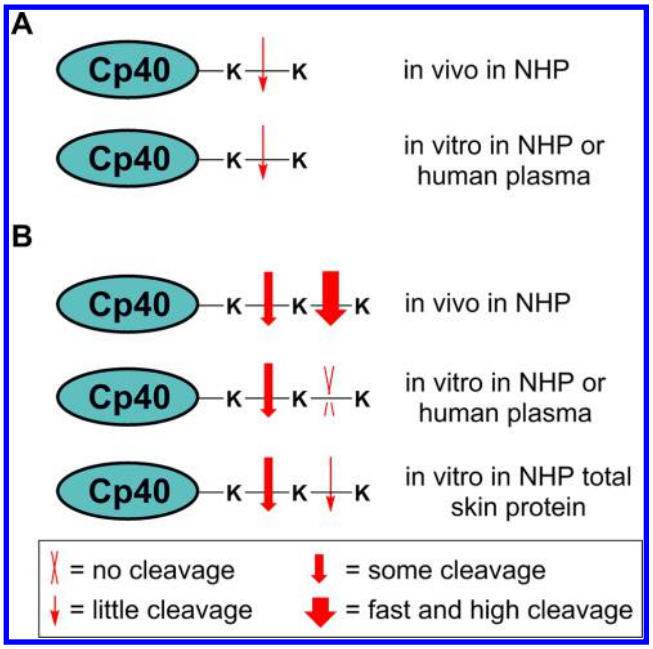

Figure 3. Schematics showing cleavage of Lys residues from Cp40-KK (A) and Cp40-KKK (B) observed in vitro and in vivo.

plasma showed preferential cleavage of Cp40-KKK to Cp40-K (Figure 3). Interestingly, incubation of Cp40-KKK with a preparation of proteins extracted from the skin of NHPs resulted in Cp40-K fragments (Figure 3), indicating that Lys-Lys bonds are cleaved both in the subcutaneous compartment and in the circulation. Further investigation is therefore required to identify the Lys-cleaving enzyme and assess the biological relevance of this phenomenon.

CONCLUSION

Novel analogs of the C3 inhibitor Cp40 were developed by attaching low molecular weight PEG chains to the Cp40 N-terminus or Lys residues to the C-terminus. The compounds mPEG(3k)-Cp40, Cp40-KK, and Cp40-KKK showed a drastic improvement in their solubility (>200-fold) at physiological pH when compared to the parental peptide, Cp40. Most importantly, the novel analogs maintained inhibitory activity and showed improved pharmacokinetic profiles when compared to Cp40. In vivo studies in which non-human primates were administered sc with 2 mg/kg of the individual analogs indicated that mPEG(3k)-Cp40 had a higher C_{max} (~2-fold), longer C3 saturation time (~34 h), longer $t_{1/2}$ by ~15 h, increased AUC_{0-120h} (~2.7-fold), and decreased CL/F (~3-fold) than did the parental compound. Among the analogs with additional residues of Lys, Cp40-KK and Cp40-KKK appeared to be the most promising compounds. Pharmacokinetic studies showed that Cp40-KK was associated with a higher $t_{1/2}$ (~5-fold), higher C_{max} (~2-fold), and decreased CL/F (~2.6-fold) when compared to Cp40. Cp40-KKK, in turn, had a higher C_{max} (~2-fold), longer C3 saturation (~42 h), increased AUC_{0-120h} (~2.6-fold), and decreased CL/F (~3-fold). The overall improvement in solubility and pharmacokinetic profile associated with these novel analogs, bolstered by their potential to reduce the frequency of drug administration and minimize any local irritation at the injection site, makes them attractive C3-targeted therapeutic candidates for treatment of chronic diseases associated with imbalanced complement activation.

EXPERIMENTAL SECTION

Reagents. Acetic acid, acetonitrile (LC/MS grade), ammonium acetate, bovine serum albumin, dichloromethane (DCM), diethyl ether, dimethylformamide (DMF), formic acid (FA), and methanol (LC/MS grade) were purchased from Fisher Scientific. Trifluoroacetic acid (TFA) was obtained from Alfa Aesar (Tewksbury, MA), methyl-PEG_{12}-NHS ester (mPEG(528)-NHS ester) and methyl-PEG_{24}-NHS ester (mPEG(1056)-NHS ester) were from Thermo Scientific, mPEG-SCM-3000 (mPEG(3k)-NHS ester) and mPEG-SCM-2000 (mPEG(2k)-NHS ester) were from JenKem Technology USA Inc. (Plano, TX), and mPEG-SCM-1000 (mPEG(1k)-NHS ester) was from Creative PEGWorks (Chapel Hill, NC). DEPBT and the Fmoc-protected amino acids Cys(Acm), His(Trt), Ala, Sar, Trp(Boc), Gln(Trt), Val, Cys(Trt), Ile, and D-Tyr(^{t}Bu) were purchased from Novabiochem (San Diego, CA). Rink amide MBHA resin (200–400 mesh) and Fmoc-Me-Ile-OH were obtained from Peptides International (Louisville, KY), Fmoc-Arg(Pbf)-OH was from AAPPTec (Louisville, KY), and HOAt was from Advanced ChemTec (Louisville, KY). ABTS (2,2′-azino-bis(3-ethylbenzothiazoline-6-sulfonic acid) was obtained from Roche (Mannheim, Germany), peroxidase-conjugated goat IgG fraction to human complement C3 was from MP Biomedicals, LLC (Solon, OH), and rabbit anti-ova polyclonal antibody was produced by Cocalico Biologicals (Steven, PA). All other reagents were purchased from Sigma-Aldrich (St. Louis, MO).

Analytical Methods. Characterization, including purity determination, of the peptides was performed with analytical reversed-phase high-performance liquid chromatography (RP-HPLC, Figure S5) and matrix-assisted laser desorption ionization-time-of-flight mass spectrometry (MALDI-TOF MS, Figures S6 and S7) on a Micromass MALDI micro MX (Waters Corporation, Milford, MA). Depending on the amount of compound, an XBridge BEH C18 column (5 μm particle size, 150 mm length, Waters Corporation, Milford, MA) with either a diameter of 4.6, 10, or 19 mm was used for RP-HPLC with a flow rate of 2.5, 4.5, or 16 mL/min, respectively. Elution of the compounds was achieved with a gradient of 5–70% of 0.1% TFA in acetonitrile (buffer A) in 0.1% TFA in water (buffer B) as follows: After 1 min at 95% B, A was increased up to 50% during 18 min, followed by further increase to 70% at 20 min. After 3 min at 70% A, A was decreased to 5% within 2 min and re-equilibration was performed for 5 min, resulting in a total run time of 30 min. Purity of the tested compounds was found to be ≥95% at 280 nm (Figure S5).

Peptide Concentration. Peptides were dissolved in Milli-Q water at stock concentrations of 1 mg/mL. Concentrations of stock and working solutions were determined immediately before use with a NanoDrop 2000c spectrophotometer (Thermo Scientific, Wilmington, DE) at 280 nm using the equation conc = $A/\varepsilon\ b$ (conc = concentration, A = absorbance, ε = extinction coefficient, b = path length).

Peptide Synthesis. DTyr-Ile-[Cys-Val-Trp(Me)-Gln-Asn-Trp-Sar-Ala-His-Arg-Cys]-mIle-NH_2 (Cp40), Cp40-Lys-NH_2 (Cp40-K), Cp40-Lys-Lys-NH_2 (Cp40-KK), and Cp40-Lys-Lys-Lys-NH_2 (Cp40-KKK) were synthesized in house or by GL Biochem (Shanghai, China) using Fmoc solid phase peptide synthesis based on a procedure described previously.[18,19] Purity of the compounds was verified by RP-HPLC and MALDI-TOF MS as described above (Figures S5–S7).

The synthesis of mPEG(3k)-, mPEG(2k)-, mPEG(1k)-, and mPEG(1056)-Cp40 was carried out based on PEGylation procedures described elsewhere.[28,45] In brief, 1 equiv of Cp40 (5 mg/mL) was dissolved in acetonitrile/water (1:1), and an amount of 2 equiv of the respective activated mPEG ester was added. The pH of the reaction mixture was adjusted to 8 using *N*-methylmorpholine. After stirring for 0.5–1 h at room temperature, the reaction mixture was quenched upon addition of 0.1% aqueous TFA (pH 2). All peptides were purified by RP-HPLC as described above and characterized by MALDI-TOF MS.

Of note, whereas PEGylation using polydisperse PEGs and mPEG(1056) was carried out with presynthesized Cp40, PEGylation

DOI: 10.1021/acs.jmedchem.8b00560
J. Med. Chem. 2018, 61, 6153–6162

of the monodisperse compound mPEG(528)-Cp40 was carried out on resin, eliminating one additional step of HPLC purification. For the preparation of mPEG(528)-Cp40, linear Cp40 was synthesized on resin as described previously.[18,19] After Fmoc-deprotection of the final N-terminal amino acid Fmoc-DTyr(*t*Bu)-OH by use of 20% piperidine in DMF, an amount of 3 equiv of mPEG(528)-NHS ester in DMF was added to the dried beads. The pH was adjusted to 8.0 using *N*-methylmorpholine, and agitation was allowed to proceed for 2 h on a rotator. Reaction completion was confirmed by Kaiser test. The beads were subsequently washed with DMF and DCM and dried under vacuum. The peptide was cleaved from resin as described by Qu et al.[19] The lyophilized crude linear deprotected peptide (1 equiv) was dissolved in 80% aqueous methanol, and 20 mM iodine (13 equiv) in methanol was slowly added with vigorous stirring. After 30 min of stirring at room temperature, the cyclization reaction was quenched by the addition of 20 mM aqueous ascorbic acid. Methanol was removed under reduced pressure and the crude peptide was purified by RP-HPLC as described above. The peptide was then characterized by MALDI-TOF MS (Figure S6E).

All peptides were initially obtained as a TFA salt and further converted into an acetate salt on the HPLC column using 25 mM aqueous ammonium acetate.[46] To this end, an XBridge BEH C18 column (5 μm particle size, 150 mm length, 19 mm diameter, Waters Corporation, Milford, MA) was equilibrated at a flow rate of 16 mL/min with a blank run, starting with 5% of 0.1% AcOH in acetonitrile (buffer C) in 0.1% AcOH in water (buffer D) for 1 min, followed by gradient increase of buffer C to 50% during 18 min, further increase to 70% at 20 min, 3 min at 70%, followed by decrease to 5% within 2 min and re-equilibration for 5 min at 5% buffer C, resulting in a total run time of 30 min. After the blank, the sample was injected and the peptide was washed on the column for 25 min with 25 mM ammonium acetate. The peptide was eluted using an elution gradient of 5−70% buffer D as described for the blank. The mass of the final compounds was confirmed by MALDI-TOF MS (Figures S6, S7). Peptides used for in vivo experiments were tested for the presence of endotoxin (<0.03 EU/mL).

Solubility Experiments. Peptide (5−10 mg) was weighed in LoBind Eppendorf tubes; an amount of 20 μL of PBS (pH 7.4) was added, and the mixture was vortexed and centrifuged for 2 min at 16 873*g*. Unless otherwise noted, if the respective peptide was not dissolved, PBS was added in portions of 10 μL, followed by vortexing and centrifugation, until all precipitate disappeared. The pH of the peptide solutions was determined on pH indicator strips or using a SevenExcellence pH meter (Mettler Toledo, Columbus, OH). The concentrations of the final solutions were determined based on the absorbance measured on a NanoDrop 2000c spectrophotometer as described above.

Complement Inhibition Assays. The ability of the Cp40 analogs to inhibit classical pathway (CP) complement activation was assessed with an established enzyme-linked immunosorbent assay (ELISA).[31] In brief, 96-well plates were coated with 50 μL of 1% ovalbumin in PBS at ambient temperature for 2 h. The wells were blocked with 200 μL of 1% BSA in PBS for 1 h, then coated with 50 μL of 1:1000 dilution of α-ovalbumin polyclonal antibody in PBS for 1 h. The plate was washed thrice with 200 μL of 0.05% Tween 20 in PBS (PBS-T) between each step. Serial dilutions of Cp40 analogs prepared in veronal buffer (VBS; 5 mM veronal, pH 7.4, containing 150 mM NaCl, 0.5 mM $CaCl_2$ and 0.5 mM $MgCl_2$) were added to a 96-well plate followed by human plasma (1:40 in VBS), and the mixture was incubated for 15 min at room temperature. After washing, complement activation (C3b/iC3b/C3d bound to the immune-complex) was detected using HRP-conjugated goat α-human C3 antibody (1:1000; MP Biomedicals). The reaction was developed using a substrate for HRP (0.05% ABTS and 0.1% of 30% H_2O_2 in 0.1 M sodium citrate, pH 4.2) and read at 405 nm using a VICTOR multilabel plate reader (PerkinElmer, Waltham, MA). The absorbance data obtained at 405 nm were converted into percentage of complement inhibition, considering that 100% complement activation is obtained in the absence of C3 peptide inhibitors. The percentage of inhibition was plotted against the logarithm of concentrations, and the resulting data set was fitted to the equation "log(inhibitor) vs normalized response" using GraphPad Prism 5 (La Jolla, CA). IC_{50} values were obtained from the fitted parameters of the mean values obtained from three independent experiments. Cp40 was always used as the internal control.

Surface Plasmon Resonance (SPR) Experiments. The binding affinity and kinetic profile of the Cp40 analogs were assessed by SPR using a Biacore 3000 instrument (GE Healthcare, Piscataway Township, NJ) based on previously described protocols.[18,19,47,48] All experiments were carried out at 25 °C using 0.01 M HEPES, pH 7.4, with 0.15 M NaCl, 3 mM EDTA, and 0.005% surfactant P20 (HBS-EP) as the running buffer. Purified human C3b (Complement Technology, Inc., Tyler, TX) was coated onto a CM5 sensor chip (GE Healthcare, Uppsala, Sweden) at densities of 11 000−20 000 resonance units (RUs) via amide coupling. A noncoated flow cell was used as a reference surface. A series of five samples of increasing concentrations (2.5, 5, 10, 20, 40 nM) of each Cp40 analog was successively injected for 2 min each at a flow rate of 30 μL/min, with a final dissociation step of 80 min. Cp40 was included in every run as an internal control. Each peptide was screened in three independent experiments. Sensorgrams were processed using Scrubber software (BioLogic Software, Campbell, Australia). The resulting data were globally fitted to a 1:1 Langmuir binding model in BIAevaluation software (GE Healthcare) to obtain the equilibrium dissociation constant (K_D) from the equation $K_D = k_d/k_a$.

Pharmacokinetic Analysis of Cp40, Cp40-KK, Cp40-KKK, and mPEG(3k)-Cp40 in Non-Human Primates (NHP). *NHP Studies and Sample Collection.* The studies were performed at the Simian Conservation Breeding and Research Center (SICONBREC), Inc. (Makati, Philippines). A total of 8 healthy male cynomolgus monkeys (*Macaca fascicularis)* with 6−7 years of age and body weight of ∼4 kg were used in this study. Prior to the study, animals were acclimatized in sterilized stainless steel cages (ILAR type 3; 600 mm × 790 mm × 780 mm) for 2 weeks in the experimental room with controlled temperature (26 ± 4 °C), relative humidity (60 ± 25%), ventilation, and a natural day and light cycle. Animals were provided daily with 100 g of food (standard monkey grower pellet, Jetstar Milling Corporation, Lipa Batangas, Philippines) and water ad libtum (via water bottle) throughout the acclimation and observation periods. A fresh banana was given daily as supplementary diet. On the day of dosing, food was provided after the administration of the compound. Each peptide analog (Cp40, Cp40-KK, Cp40-KKK, mPEG(3k)-Cp40) was administered as a single sc injection in 2 individual animals (2 animals per treatment group). Cp40 and Cp40-KK peptides (8 mg net) were reconstituted in 2 mL of sterile saline, mPEG(3k)-Cp40 was reconstituted in 0.5 mL of sterile saline and Cp40-KKK in 0.25 mL of 100 mM phosphate buffer. Subcutaneous injections were performed using a 3/10 mL insulin safety syringe with 29GX1/2 in. needle for a final dose of 2 mg/kg of peptide per animal. Blood samples were collected from the femoral vein before (0 h) and at various time points after the injection (t = 5 min, 30 min, and 1, 2, 4, 6, 12, 24, 48, 72, 96, 120 h) into EDTA-vacutainer tubes to prevent coagulation and complement activation. All blood samples were centrifuged at ∼800*g* for 10 min, and the resulting plasma samples were immediately frozen at −80 °C until use. All NHP studies were performed in accordance with institutional guidelines defined by Institutional Animal Care and Use Committee from Philippines, and U.S. SICONBREC is accredited by the international Association for Assessment and Accreditation of Laboratory Animal Care (AAALAC) for providing and maintaining a high quality program of animal care and use.

Analysis of Plasma Samples and Determination of Plasma Half-Life. (a) Preparation of Standard Solutions and Plasma Samples. Calibration curves were prepared together with the plasma samples being analyzed: Stock solutions of the respective peptide (Cp40, Cp40-KK, Cp40-KKK, or mPEG(3k)-Cp40) were spiked into untreated NHP plasma at final concentrations of 1, 2, 4, 8, and 16 μM. Prior to further analysis, all plasma samples were treated with methanol for protein precipitation[49,50] as follows: 50 μL of the NHP plasma to be analyzed was mixed in a 0.5 mL LoBind Eppendorf tube

DOI: 10.1021/acs.jmedchem.8b00560
J. Med. Chem. 2018, 61, 6153−6162

with 150 μL of methanol containing 0.5 μg/mL isotope-labeled Cp40 (DTyr-Ile-[Cys-Val-Trp(Me)-Gln-Asn-Trp-Sar-Ala-His-[$^{13}C_6$;$^{15}N_4$]Arg-Cys]-mIle-NH_2, Bachem, Torrance, CA), which served as internal standard (IS). The mixture was vortexed for ∼8 min, allowed to sit at room temperature for 10 min, and centrifuged for 20 min at 16 873*g*. The supernatant was mixed 1:1 with a solution of 20% methanol in 10 mM ammonium formate (pH 3) in an injection vial. For mPEG(3k)-Cp40 samples, 3% aqueous MeCN was used instead of the ammonium formate solution.

(b) Liquid Chromatography and Mass Spectrometry. Plasma samples were processed as described above and analyzed by ultraperformance liquid chromatography−electrospray ionization-tandem mass spectrometry (UPLC−ESI-MS) as previously described.[19,32] An Acquity UPLC system (Waters, Milford MA) with a temperature-controlled autosampler was used for the chromatographic experiments. The system was equipped with an Acquity UPLC BEH C18 VanGuard precolumn (1.7 μm, 2.1 mm × 5 mm; Waters, Milford MA) and an Acquity UPLC BEH C18 column (130 Å, 1.7 μm, 1 mm × 100 mm; Waters, Milford MA). The column temperature was kept at 40 °C and that of the autosampler at 4 °C. The injection volume was 5 μL, and all samples were analyzed in triplicate. Elution of the analytes was achieved with a gradient of 0.1% formic acid in acetonitrile (buffer E) in 0.1% formic acid in water (buffer F) at a flow rate of 0.15 mL/min as follows: 0−2 min 3% E, 2.5 min 15% E, 7 min 55% E, 8−10 min 95% E, 10.3−16 min 3% E. Cp40 and the IS eluted after 4.90 ± 0.2 min, Cp40-K after 4.65 ± 0.2 min, Cp40-KK after 4.39 ± 0.2 min, Cp40-KKK after 4.09 ± 0.2 min, and mPEG(3k)-Cp40 after 6.43 ± 0.2 min. A SYNAPT G2-S high definition mass spectrometer in the positive ion mode was used for the ESI-MS analysis. A capillary voltage of 2 kV, cone voltage of 40 V, source temperature of 120 °C, desolvation temperature of 350 °C, and desolvation gas with a flow rate of 600 L/h was applied. Spectra were acquired in the "sensitivity" acquisition mode of the instrument with ESI positive polarity settings in a range of 250−1400 m/z and a scan time of 1 s. Data acquisition and analysis were performed using MassLynx V4.1 (Waters, Milford, MA) with a mass window of ±0.1. The method was slightly adjusted for the analysis of plasma samples containing mPEG(3k)-Cp40. Here, a fixed collision energy of 35 V was applied in the ion trap. For the preparation of standard curves, the areas under the curve (AUCs) of the respective MS peaks (triple-charged Cp40 (596.97 m/z) and isotope-labeled Cp40 (600.31 m/z), quadruple-charged Cp40-K (fragment; 480.25 m/z), Cp40-KK (512.27 m/z), and Cp40-KKK (544.05 m/z), and the monocharged fragment at 436.256 m/z of mPEG(3k)-Cp40 (-Sar-Ala-His-Arg-)) were determined by integration of the peaks in the base peak intensity (BPI) chromatograms and plotted against the concentration. The plasma concentration at each time point $C(t)$ was calculated from the extracted peak area of the same mass peaks of each peptide using the corresponding standard curve.

(c) Determination of Plasma Half-Life and Additional Pharmacokinetic Parameters.[51] The elimination rate constant k_{el} and the terminal half-life $t_{1/2}$ of the peptides in NHP plasma were determined as described,[19,32] using the slope of the terminal elimination phase (t = 72−120 h) with the following equations: $\ln[C(t)] = \ln[C(t_0)] - k_{el}t$, and $t_{1/2} = \ln(2)/k_{el}$. The maximum concentration C_{max} and time of maximum concentration observed (t_{max}) were determined manually from the pharmacokinetic profiles. The area under the curve AUC from 0 to 120 h (AUC_{0-t}), AUC from 0 to infinity ($AUC_{0-\infty}$), the apparent volume of distribution Vz/F (F = bioavailability), and the apparent clearance CL/F were calculated using the following equations: $AUC_{0-t_n} = \int_0^{t_n} C(t)\,dt$, $AUC_{0-\infty} = AUC_{0-t} + AUC_{t-\infty}$, $Vz/F = CL/k_{el}$, $CL/F = DOSE/AUC_{0-\infty}$, with t_n = 120 h. All pharmacokinetic parameters were calculated using a noncompartmental approach with Phoenix WinNonlin 8.0 (Certara L.P. (Pharsight), St. Louis, MO). The plasma model (extravascular dosing) was used with linear trapezoidal linear interpolation.

Assessment of C3 Levels in NHP Plasma. Immunonephelometry was carried out to determine the levels of complement component C3 in NHP plasma as previously described.[32]

Assessment of Proteolysis of Cp40-KK and Cp40-KKK. Cp40-KK or Cp40-KKK was spiked into either NHP or human plasma at a final concentration of 16 μM. Cp40-KKK was also spiked into NHP skin total protein (from cynomolgus monkeys; Zyagen, San Diego, CA) to a final concentration of 20 μM. The samples were incubated for 24 h at 37 °C in a water bath, and samples were taken before and at various time points during and at the end of the incubation. The samples were subjected to protein precipitation as described above and analyzed by UPLC−ESI MS as described above.

■ ASSOCIATED CONTENT

Supporting Information

The Supporting Information is available free of charge on the ACS Publications website at DOI: 10.1021/acs.jmedchem.8b00560.

Additional figures illustrating inhibition data, SPR binding profiles, pharmacokinetic data, HPLC traces, and MALDI spectra (PDF)

■ AUTHOR INFORMATION

Corresponding Author

*E-mail: lambris@pennmedicine.upenn.edu.

ORCID

John D. Lambris: 0000-0002-9370-5776

Notes

The authors declare the following competing financial interest(s): J.D.L. is the founder of Amyndas Pharmaceuticals, which is developing complement inhibitors (including third-generation compstatin analogues such as AMY-101), and inventor of patents or patent applications that describe the use of complement inhibitors for therapeutic purposes, some of which are developed by Amyndas Pharmaceuticals. J.D.L. is also the inventor of the compstatin technology licensed to Apellis Pharmaceuticals (4(1MeW)7W, also known as POT-4 and APL-1) and PEGylated derivatives such as APL-2.

■ ACKNOWLEDGMENTS

We thank Deborah McClellan for editorial assistance, Dimitrios C. Mastellos for critical review of the manuscript, and Corinne Seng-Yue from Learn and Confirm for assistance in the pharmacokinetic analysis. This work was supported by grants from the U.S. National Institutes of Health (Grants AI068730, AI030040) and by funding from the European Community's Seventh Framework Programme, under Grant Agreement 602699 (DIREKT).

■ ABBREVIATIONS USED

AMD, age-related macular degeneration;; CL/F, apparent clearance; C_{max}, maximum concentration; CP, classical pathway; Da, dalton; F, bioavailability; k_a, association constant; k_d, dissociation constant; k_{el}, elimination rate constant; K_D, equilibrium dissociation constant; NHP, non-human primate; PNH, paroxysmal nocturnal hemoglobinuria; SPR, surface plasmon resonance; $t_{1/2}$, terminal half-life; t_{max}, time of maximum concentration observed; Vz/F, apparent volume of distribution.

■ REFERENCES

(1) Hajishengallis, G.; Reis, E. S.; Mastellos, D. C.; Ricklin, D.; Lambris, J. D. Novel mechanisms and functions of complement. *Nat. Immunol.* **2017**, *18*, 1288−1298.

DOI: 10.1021/acs.jmedchem.8b00560
J. Med. Chem. 2018, 61, 6153−6162

(2) Reis, E. S.; Mastellos, D. C.; Ricklin, D.; Mantovani, A.; Lambris, J. D. Complement in cancer: untangling an intricate relationship. *Nat. Rev. Immunol.* **2018**, *18*, 5−18.
(3) Legendre, C.; Sberro-Soussan, R.; Zuber, J.; Fremeaux-Bacchi, V. The role of complement inhibition in kidney transplantation. *Br. Med. Bull.* **2017**, 1−13.
(4) Ricklin, D.; Reis, E. S.; Lambris, J. D. Complement in disease: a defence system turning offensive. *Nat. Rev. Nephrol.* **2016**, *12*, 383−401.
(5) Sina, C.; Kemper, C.; Derer, S. The intestinal complement system in inflammatory bowel disease: shaping intestinal barrier function. *Semin. Immunol.* **2018**, *37*, 66−73.
(6) Nording, H.; Langer, H. F. Complement links platelets to innate immunity. *Semin. Immunol.* **2018**, *37*, 43−52.
(7) Mödinger, Y.; Löffler, B.; Huber-Lang, M.; Ignatius, A. Complement involvement in bone homeostasis and bone disorders. *Semin. Immunol.* **2018**, *37*, 53−65.
(8) Wong, E. K. S.; Kavanagh, D. Diseases of complement dysregulation—an overview. *Semin. Immunopathol.* **2018**, *40*, 49−64.
(9) Rother, R. P.; Rollins, S. A.; Mojcik, C. F.; Brodsky, R. A.; Bell, L. Discovery and development of the complement inhibitor eculizumab for the treatment of paroxysmal nocturnal hemoglobinuria. *Nat. Biotechnol.* **2007**, *25*, 1256−1264.
(10) Thomas, T. C.; Rollins, S. A.; Rother, R. P.; Giannoni, M. A.; Hartman, S. A.; Elliott, E. A.; Nye, S. H.; Matis, L. A.; Squinto, S. P.; Evans, M. J. Inhibition of complement activity by humanized anti-C5 antibody and single-chain Fv. *Mol. Immunol.* **1996**, *33*, 1389−1401.
(11) Ricklin, D.; Mastellos, D. C.; Reis, E. S.; Lambris, J. D. The renaissance of complement therapeutics. *Nat. Rev. Nephrol.* **2018**, *14*, 26−47.
(12) Ricklin, D.; Barratt-Due, A.; Mollnes, T. E. Complement in clinical medicine: clinical trials, case reports and therapy monitoring. *Mol. Immunol.* **2017**, *89*, 10−21.
(13) Harris, C. L. Expanding horizons in complement drug discovery: challenges and emerging strategies. *Semin. Immunopathol.* **2018**, *40*, 125−140.
(14) Risitano, A. M.; Marotta, S. Toward complement inhibition 2.0: next generation anticomplement agents for paroxysmal nocturnal hemoglobinuria. *Am. J. Hematol.* **2018**, *93*, 564−577.
(15) Mastellos, D. C.; Yancopoulou, D.; Kokkinos, P.; Huber-Lang, M.; Hajishengallis, G.; Biglarnia, A. R.; Lupu, F.; Nilsson, B.; Risitano, A. M.; Ricklin, D.; Lambris, J. D. Compstatin: a C3-targeted complement inhibitor reaching its prime for bedside intervention. *Eur. J. Clin. Invest.* **2015**, *45*, 423−440.
(16) Sahu, A.; Kay, B. K.; Lambris, J. D. Inhibition of human complement by a C3-binding peptide isolated from a phage-displayed random peptide library. *J. Immunol.* **1996**, *157*, 884−891.
(17) Huang, Y. Evolution of compstatin family as therapeutic complement inhibitors. *Expert Opin. Drug Discovery* **2018**, *13*, 435−444.
(18) Qu, H.; Magotti, P.; Ricklin, D.; Wu, E. L.; Kourtzelis, I.; Wu, Y. Q.; Kaznessis, Y. N.; Lambris, J. D. Novel analogues of the therapeutic complement inhibitor compstatin with significantly improved affinity and potency. *Mol. Immunol.* **2011**, *48*, 481−489.
(19) Qu, H.; Ricklin, D.; Bai, H.; Chen, H.; Reis, E. S.; Maciejewski, M.; Tzekou, A.; DeAngelis, R. A.; Resuello, R. R.; Lupu, F.; Barlow, P. N.; Lambris, J. D. New analogs of the clinical complement inhibitor compstatin with subnanomolar affinity and enhanced pharmacokinetic properties. *Immunobiology* **2013**, *218*, 496−505.
(20) Mastellos, D. C.; Reis, E. S.; Ricklin, D.; Smith, R. J.; Lambris, J. D. Complement C3-targeted therapy: replacing long-held assertions with evidence-based discovery. *Trends Immunol.* **2017**, *38*, 383−394.
(21) van Griensven, M.; Ricklin, D.; Denk, S.; Halbgebauer, R.; Braun, C. K.; Schultze, A.; Hones, F.; Koutsogiannaki, S.; Primikyri, A.; Reis, E.; Messerer, D.; Hafner, S.; Radermacher, P.; Biglarnia, A. R.; Resuello, R. R. G.; Tuplano, J. V.; Mayer, B.; Nilsson, K.; Nilsson, B.; Lambris, J. D.; Huber-Lang, M. Protective effects of the complement inhibitor compstatin Cp40 in hemorrhagic shock. *Shock* [Online early access] DOI: 10.1097/SHK.0000000000001127. Published Online: February 14, **2018**.
(22) Katragadda, M.; Magotti, P.; Sfyroera, G.; Lambris, J. D. Hydrophobic effect and hydrogen bonds account for the improved activity of a complement inhibitor, compstatin. *J. Med. Chem.* **2006**, *49*, 4616−4622.
(23) Kaushal, S.; Grossi, F.; Francois, C.; Slakter, J.; Group, A. S. Complement C3 inhibitor POT-4: clinical safety of intravitreal administration. *Invest. Ophthalmol. Visual Sci.* **2009**, *50*, 5010.
(24) Francois, C.; Deschatelets, P. Cell-Reactive, Long-Acting, or Targeted Compstatin Analogs and Related Compositions and Methods. U.S. Patent Appl. 2016/0215020 A1, July 28, 2016.
(25) U.S. National Library of Medicine. ClinicalTrials.gov. https://clinicaltrials.gov/show/NCT03226678 (accessed 2017).
(26) U.S. National Library of Medicine. ClinicalTrials.gov. https://clinicaltrials.gov/ct2/show/NCT03453619 (accessed 2018).
(27) Janssen, B. J.; Halff, E. F.; Lambris, J. D.; Gros, P. Structure of compstatin in complex with complement component C3c reveals a new mechanism of complement inhibition. *J. Biol. Chem.* **2007**, *282*, 29241−29247.
(28) Risitano, A. M.; Ricklin, D.; Huang, Y.; Reis, E. S.; Chen, H.; Ricci, P.; Lin, Z.; Pascariello, C.; Raia, M.; Sica, M.; Del Vecchio, L.; Pane, F.; Lupu, F.; Notaro, R.; Resuello, R. R.; DeAngelis, R. A.; Lambris, J. D. Peptide inhibitors of C3 activation as a novel strategy of complement inhibition for the treatment of paroxysmal nocturnal hemoglobinuria. *Blood* **2014**, *123*, 2094−2101.
(29) Veronese, F. M. Peptide and protein PEGylation: a review of problems and solutions. *Biomaterials* **2001**, *22*, 405−417.
(30) Kato, A.; Maki, K.; Ebina, T.; Kuwajima, K.; Soda, K.; Kuroda, Y. Mutational analysis of protein solubility enhancement using short peptide tags. *Biopolymers* **2007**, *85*, 12−18.
(31) Mallik, B.; Katragadda, M.; Spruce, L. A.; Carafides, C.; Tsokos, C. G.; Morikis, D.; Lambris, J. D. Design and NMR characterization of active analogues of compstatin containing non-natural amino acids. *J. Med. Chem.* **2005**, *48*, 274−286.
(32) Primikyri, A.; Papanastasiou, M.; Sarigiannis, Y.; Koutsogiannaki, S.; Reis, E. S.; Tuplano, J. V.; Resuello, R. R.; Nilsson, B.; Ricklin, D.; Lambris, J. D. Method development and validation for the quantitation of the complement inhibitor Cp40 in human and cynomolgus monkey plasma by UPLC-ESI-MS. *J. Chromatogr. B: Anal. Technol. Biomed. Life Sci.* **2017**, *1041−1042*, 19−26.
(33) Thapa, R. K.; Choi, H.-G.; Kim, J. O.; Yong, C. S. Analysis and optimization of drug solubility to improve pharmacokinetics. *J. Pharm. Invest.* **2017**, *47*, 95−110.
(34) Gorham, R. D.; Forest, D. L.; Khoury, G. A.; Smadbeck, J.; Beecher, C. N.; Healy, E. D.; Tamamis, P.; Archontis, G.; Larive, C. K.; Floudas, C. A.; Radeke, M. J.; Johnson, L. V.; Morikis, D. New compstatin peptides containing N-terminal extensions and non-natural amino acids exhibit potent complement inhibition and improved solubility characteristics. *J. Med. Chem.* **2015**, *58*, 814−826.
(35) Bockus, A. T.; Schwochert, J. A.; Pye, C. R.; Townsend, C. E.; Sok, V.; Bednarek, M. A.; Lokey, R. S. Going out on a limb: delineating the effects of β-branching, N-methylation, and side chain size on the passive permeability, solubility, and flexibility of sanguinamide A analogues. *J. Med. Chem.* **2015**, *58*, 7409−7418.
(36) Gorham, R. D.; Forest, D. L.; Tamamis, P.; López de Victoria, A.; Kraszni, M.; Kieslich, C. A.; Banna, C. D.; Bellows-Peterson, M. L.; Larive, C. K.; Floudas, C. A.; Archontis, G.; Johnson, L. V.; Morikis, D. Novel compstatin family peptides inhibit complement activation by drusen-like deposits in human retinal pigmented epithelial cell cultures. *Exp. Eye Res.* **2013**, *116*, 96−108.
(37) Mohan, R. R.; Cabrera, A. P.; Harrison, R. E. S.; Gorham, R. D.; Johnson, L. V.; Ghosh, K.; Morikis, D. Peptide redesign for inhibition of the complement system: targeting age-related macular degeneration. *Mol. Vision* **2016**, *22*, 1280−1290.
(38) Mero, A.; Spolaore, B.; Veronese, F. M.; Fontana, A. Transglutaminase-mediated PEGylation of proteins: direct identification of the sites of protein modification by mass spectrometry

DOI: 10.1021/acs.jmedchem.8b00560
J. Med. Chem. 2018, 61, 6153−6162

using a novel monodisperse PEG. *Bioconjugate Chem.* **2009**, *20*, 384−389.
(39) Maiser, B.; Dismer, F.; Hubbuch, J. Optimization of random PEGylation reactions by means of high throughput screening. *Biotechnol. Bioeng.* **2014**, *111*, 104−114.
(40) Zhang, F.; Liu, M.-r.; Wan, H.-t. Discussion about several potential drawbacks of PEGylated therapeutic proteins. *Biol. Pharm. Bull.* **2014**, *37*, 335−339.
(41) Ivens, I. A.; Achanzar, W.; Baumann, A.; Brandli-Baiocco, A.; Cavagnaro, J.; Dempster, M.; Depelchin, B. O.; Irizarry Rovira, A. R.; Dill-Morton, L.; Lane, J. H.; Reipert, B. M.; Salcedo, T.; Schweighardt, B.; Tsuruda, L. S.; Turecek, P. L.; Sims, J. PEGylated biopharmaceuticals: current experience and considerations for nonclinical development. *Toxicol. Pathol.* **2015**, *43*, 959−983.
(42) Verhoef, J. J.; Carpenter, J. F.; Anchordoquy, T. J.; Schellekens, H. Potential induction of anti-PEG antibodies and complement activation toward PEGylated therapeutics. *Drug Discovery Today* **2014**, *19*, 1945−1952.
(43) Zhang, P.; Sun, F.; Liu, S.; Jiang, S. Anti-PEG antibodies in the clinic: current issues and beyond PEGylation. *J. Controlled Release* **2016**, *244*, 184−193.
(44) Zhang, X.; Wang, H.; Ma, Z.; Wu, B. Effects of pharmaceutical PEGylation on drug metabolism and its clinical concerns. *Expert Opin. Drug Metab. Toxicol.* **2014**, *10*, 1691−1702.
(45) Wahren, J.; Barrack, S.; Callaway, J.; Mazzoni, M.; Foyt, H.; Daniels, M. PEGylated C-Peptide. U.S. Pat. Appl. 2013/0130973 A1, May 23, 2013.
(46) Tovi, A.; Eidelman, C.; Sushan, S.; Elster, S.; Alon, H.; Ivchenko, A.; Butilca, G.-M.; Zaoui, G. A Counterion Exchange Process for Peptides. Eur. Pat. Appl. EP1709065 A2, October 11, 2006.
(47) Magotti, P.; Ricklin, D.; Qu, H.; Wu, Y. Q.; Kaznessis, Y. N.; Lambris, J. D. Structure-kinetic relationship analysis of the therapeutic complement inhibitor compstatin. *J. Mol. Recognit.* **2009**, *22*, 495−505.
(48) Huang, Y.; Reis, E. S.; Knerr, P. J.; van der Donk, W. A.; Ricklin, D.; Lambris, J. D. Conjugation to albumin-binding molecule tags as a strategy to improve both efficacy and pharmacokinetic properties of the complement inhibitor compstatin. *ChemMedChem* **2014**, *9*, 2223−2226.
(49) Bruce, S. J.; Tavazzi, I.; Parisod, V.; Rezzi, S.; Kochhar, S.; Guy, P. A. Investigation of human blood plasma sample preparation for performing metabolomics using ultrahigh performance liquid chromatography/mass spectrometry. *Anal. Chem.* **2009**, *81*, 3285−3296.
(50) Rico, E.; Gonzalez, O.; Blanco, M. E.; Alonso, R. M. Evaluation of human plasma sample preparation protocols for untargeted metabolic profiles analyzed by UHPLC-ESI-TOF-MS. *Anal. Bioanal. Chem.* **2014**, *406*, 7641−7652.
(51) Gabrielsson, J.; Weiner, D. *Pharmacokinetic and Pharmacodynamic Data Analysis: Concepts and Applications*, 4th ed.; Swedish Pharmaceutical Press: Stockholm, Sweden, 2007.

DOI: 10.1021/acs.jmedchem.8b00560
J. Med. Chem. 2018, 61, 6153−6162